energies

MDPI

Article

Comparative Assessment of sCO2 Cycles, Optimal ORC, and Thermoelectric Generators for Exhaust Waste Heat Recovery Applications from Heavy-Duty Diesel Engines

Menaz Ahamed [1], Apostolos Pesyridis [1], Jabraeil Ahbabi Saray [2], Amin Mahmoudzadeh Andwari [1,3,*], Ayat Gharehghani [2,*] and Srithar Rajoo [4]

[1] Department of Mechanical and Aerospace Engineering, Brunel University, London UB8 3PH, UK; 1500388@brunel.ac.uk (M.A.); a.pesyridis@brunel.ac.uk (A.P.)
[2] School of Mechanical Engineering, Iran University of Science and Technology, Narmak, Tehran 16846, Iran; j_ahbabi@mecheng.iust.ac.ir
[3] Machine and Vehicle Design (MVD), Materials and Mechanical Engineering, Faculty of Technology, University of Oulu, FI-90014 Oulu, Finland
[4] UTM Centre for Low Carbon Transport (LoCARtic), IVeSE, Universiti Teknologi Malaysia, Skudai 81310, Johor, Malaysia; srithar@utm.my
* Correspondence: amiN·mahmoudzadehandwari@oulu.fi (A.M.A.); ayat_gharehghani@iust.ac.ir (A.G.)

Abstract: This study aimed to investigate the potential of supercritical carbon dioxide (sCO2), organic Rankine cycle (ORC), and thermoelectric generator (TEG) systems for application in automotive exhaust waste heat recovery (WHR) applications. More specifically, this paper focuses on heavy-duty diesel engines applications such as marine, trucks, and locomotives. The results of the simulations show that sCO2 systems are capable of recovering the highest amount of power from exhaust gases, followed by ORC systems. The sCO2 system recovered 19.5 kW at the point of maximum brake power and 10.1 kW at the point of maximum torque. Similarly, the ORC system recovered 14.7 kW at the point of maximum brake power and 7.9 kW at the point of maximum torque. Furthermore, at a point of low power and torque, the sCO2 system recovered 4.2 kW of power and the ORC system recovered 3.3 kW. The TEG system produced significantly less power (533 W at maximum brake power, 126 W at maximum torque, and 7 W at low power and torque) at all three points of interest due to the low system efficiency in comparison to sCO2 and ORC systems. From the results, it can be concluded that sCO2 and ORC systems have the biggest potential impact in exhaust WHR applications provided the availability of heat and that their level of complexity does not become prohibitive.

Keywords: waste heat recovery; WHR; diesel engine; organic Rankine cycle; ORC; supercritical carbon dioxide; sCO2; thermoelectric generator; TEG; fuel economy; fuel efficiency; fuel consumption reduction

Citation: Ahamed, M.; Pesyridis, A.; Ahbabi Saray, J.; Mahmoudzadeh Andwari, A.; Gharehghani, A.; Rajoo, S. Comparative Assessment of sCO2 Cycles, Optimal ORC, and Thermoelectric Generators for Exhaust Waste Heat Recovery Applications from Heavy-Duty Diesel Engines. *Energies* **2023**, *16*, 4339. https://doi.org/10.3390/en16114339

Academic Editors: Georgios Mavropoulos, E.C. Andritsakis and Roussos G. Papagiannakis

Received: 19 April 2023
Revised: 21 May 2023
Accepted: 24 May 2023
Published: 25 May 2023

1. Introduction

Diesel engines were widely used for heavy goods transportation, agriculture, and industrial machines for many decades. However, with growing pressure from environmental groups and government regulation, automotive manufacturers are being forced to improve engine efficiency and reduce fuel consumption, consequently leading to reduced CO_2 and other greenhouse gas (GHG) emissions into the atmosphere. Figure 1 shows the typical energy losses in a heavy-duty diesel engine. As can be seen in the diagram, over half of the fuel energy is wasted mainly through exhaust and cooling systems [1]. A waste heat recovery system has the potential to convert some of this wasted energy into electricity, which can be used to reduce the load on the vehicle alternator or power auxiliary components, such as the air conditioning and lights [2,3]. Therefore, fuel consumption can be reduced.

There are three promising systems that are being investigated currently in the industry for use in automotive exhaust waste heat recovery applications. These are the thermoelectric generators (TEGs), the organic Rankine cycle (ORC)-based systems, and supercritical carbon dioxide (sCO2)-based systems [4–7]. These systems can not only be used for exhaust heat recovery, but also in many other industries, such as nuclear power generation, fossil fuel power generation, and shipboard power. These were specifically chosen as they are at the highest state of technological readiness compared to newer option (thermo-acoustic systems, for example) available that are under early to mid-stage research.

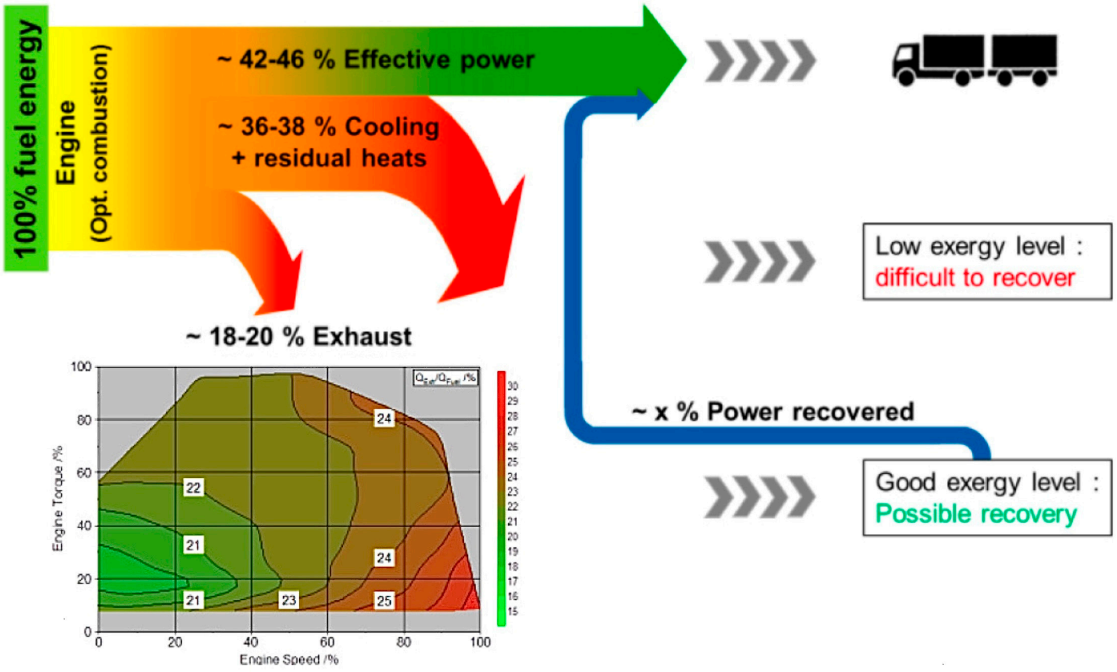

Figure 1. Typical energy losses in heavy-duty diesel engines [5].

1.1. Supercritical Carbon Dioxide (sCO2) Cycles

CO2 is an environmentally benign natural working fluid that is inexpensive, non-flammable, non-explosive, and abundant in nature. Furthermore, it has a low global warming potential (GWP) and no ozone-depleting potential (ODP) [8–11], which are important environmental characteristics when selecting the working fluid for a thermodynamic power generation cycle. The layout of these waste heat recovery systems can be seen in Figure 2 below.

As CO2 approaches its critical point, it becomes more incompressible; therefore, the compressor work can be decreased substantially, leading to higher thermodynamic cycle efficiencies. Another benefit of using sCO2 cycles is that they operate at much higher pressures throughout the cycle, which results in a higher density working fluid, thereby facilitating smaller equipment sizes and physical footprint, and hence lower capital cost [12].

Due to the compact nature of these systems, their environmentally friendly characteristics, safety levels, and the properties of the working fluid, sCO2 cycles emerged as a promising method in engine waste heat recovery. The technical feasibility of using CO2-based systems in engine waste heat recovery was already verified as it is already being used in vehicle air conditioning systems [13–16].

Manjunath et al. carried out a study on sCO2 waste heat recovery cycles for shipboard power applications. The study compared a proposed system that uses the sCO2 Brayton cycle to a conventional topping Brayton cycle that is already used for the application. They found that an increase in power output of around 18% can be achieved, as well as an increase in the overall shipboard power system efficiency of more than 11% [17]. Song

et al. carried out a simulation study to test the performance improvement of a preheating sCO2 cycle-based system for engine waste heat recovery. The engine in consideration was an inline six turbocharged diesel engine that was used previously for ORC waste heat recovery studies. The results from the simulation show that the improved system can better utilize the regeneration heat load and hence improve system performance. Moreover, the maximum net output of the system is 7.4% higher than the original system. By adopting the improved preheating system, the engine power output was increased by 6.9% [1]. Furthermore, a similar study carried on the same engine with similar sCO2-based systems found that the engine power output was increased by 8.5%, indicating a tremendous potential for practical applications [1].

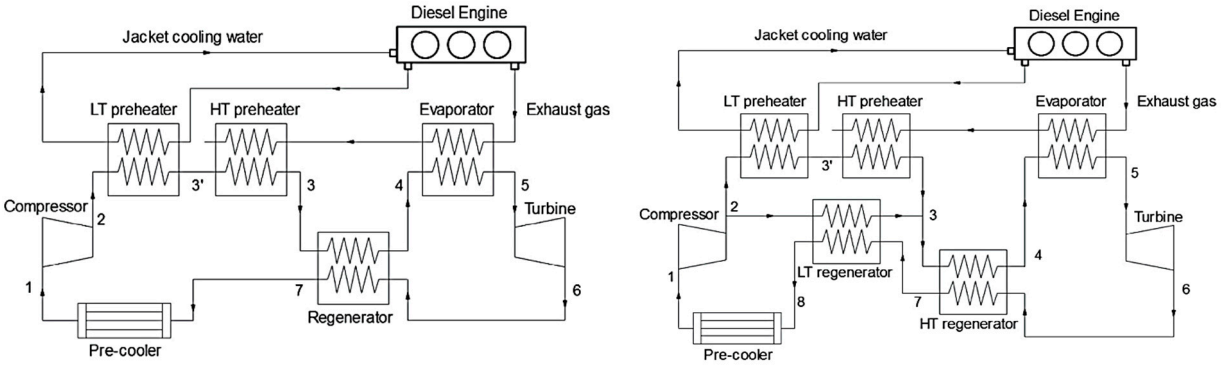

(a) Original preheating S-CO_2 cycle based system (b) Improved S-CO_2 cycle based system with a regeneration branch

Figure 2. (**a**) Original preheating sCO2 system and (**b**) improved sCO2 system with regeneration branch [17].

The cost of sCO2 systems varies significantly with the architecture of the system. Marchionni et al. studied the cost of various sCO2 architectures (in the 160–175 kWe range). They found that the simple recompression and simple recuperation layouts have investment costs of USD/kWe 1175 and USD/kWe 862.5, respectively. More complex systems such as the recompression, reheating layout can have costs as high as USD/kWe 1675 [18].

1.2. Organic Rankine Cycle (ORC)

ORC waste heat recovery systems were heavily investigated for application in heavy-duty diesel engines for several decades. Mahmoudi et al. carried out an extensive literature review on ORC research. They found that diesel engines and gas turbines are the most used heat sources for WHR studies [19]. The layout of the system onboard diesel engine with exhaust gas recirculation (EGR) can be seen in Figure 3 below.

One of the first studies carried out was by Teng et al. who simulated an ORC WHR system on a Cummins ISX heavy-duty diesel engine with a rated brake power of 275 kW. The results of the simulations show that 55 kW of mechanical work was recovered by the ORC WHR system in steady-state conditions, which is equivalent to about a 20% increase in engine power without any additional fuel consumption [20]. Moreover, the efficiency of the ORC system was found to be 29.5% [20]. Another study carried out by Cipollone et al. tested an IVECO N67 engine operating at 1500 rpm and 25% load (a brake power of 35 kW). The ORC system was able to recover 2 kW of electric power at this power range [21]. Additionally, Pesyridis et al. carried out a study on a 10.3 L, 316 kW turbocharged heavy-duty diesel engine using an ORC WHR system. The system was able to recover 2–4 kW at low speeds and 8–16 kW at high speeds [22,23]. Moreover, Arunachalam et al. simulated an ORC WHR system on a 13 L, 367 kW Volvo D-13 engine using a mixture of 80% water and 20% ethanol as the working fluid. They found that the efficiency of the WHR system varied between 9 and 23% depending on the source of the waste heat [24]. Moreover, Varshil and Deshmouk [25] reviewed ORC performance for diesel engines of various configurations

and found that there is a potential of improving fuel economy by up to 5% through effective implementation of ORC systems for waste heat recovery.

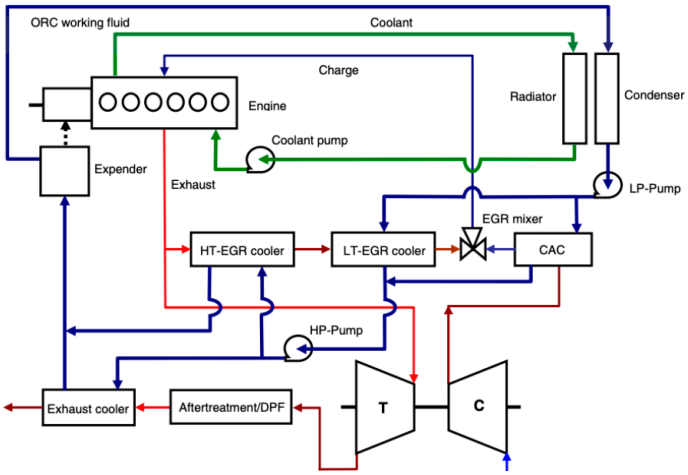

Figure 3. ORC WHR system with integrated low-temperature cooling loop [20].

The focus more recently was on investigating the fuel economy potential of using ORC WHR systems. An experiment based on a 10.8 L 2006-MY Cummins ISM diesel engine in typical driving conditions was carried out by Teng et al. [26]. Thermodynamic analysis showed that up to a 5% fuel economy improvement was achieved using the WHR system above. Moreover, Laouid et al. conducted a multi-objective optimization of different organic Rankine cycle configurations and also found fuel economy improvements of 5–8.78%, with the latter being obtained by an ORC with an internal heat exchanger [27]. Hoang carried out an extensive review on ORC WHR diesel engine studies. He found that up to a 10% fuel saving can be achieved realistically, as well as 10–25% thermal efficiency for single-loop ORC systems and 60–90% for dual- or multi-loop ORC systems [28]. These exact findings were replicated by Chintala et al., who carried out a similar technical review on compression ignition engines using ORC WHR systems. They also found that R245fa is the best working fluid for these systems due to its good performance as a refrigerant, its availability, and its low economic and environmental impacts [29]. ORC systems were also heavily investigated for mobile marine applications. Mat Nawi et al. carried out a study using bioethanol as the working fluid in the ORC system. The results show that the ORC system was able to recover 5 kW of power from a 996 kW marine diesel engine running at 1500 rpm [30]. Moreover, Mondejar et al. found that ORC systems recovering heat from exhaust gases produced by marine diesel engines running on low-sulphur fuels could yield fuel savings of 10–15% [31]. In terms of both simulation and experimental studies, the fuel economy improvement ranges from 2 to 10%. These values depend on the design and selection of components, the working fluid used, and the architecture of the WHR system [32].

1.3. Thermoelectric Generators (TEG)

Thermoelectric processes are those the result in the direct conversion of thermal energy into electrical energy. Thermoelectric generators (TEG) have great potential to be used in waste heat recovery applications in power plants and automotive vehicles. They have many advantages, including low maintenance, zero environmental impact, silent operation, compactness, and stability. However, there are considerable technical challenges still remaining that, thus far, limited the progress of these systems. These include low efficiency and low maximum operating temperature, which are dictated by the selection of thermoelectric materials, as well as integration effects that arise from increased mass, complexity, and increased exhaust backpressure. Figure 4 below shows a typical thermoelectric module that can be used to generate electricity.

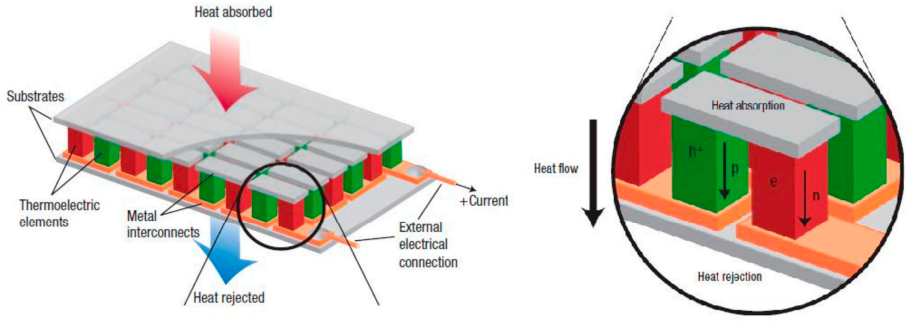

Figure 4. Working principle of thermoelectric module and its components [33].

Kumar et al. created a model for a TEG WHR system based on a General Motors prototype Chevrolet Suburban. They were able to obtain a thermoelectric efficiency of 5.5% and heat exchanger transfer efficiency of 64% [33]. Lan et al. used a novel combination of TEG with and without ORC. They were able to produce 400 W of power and claimed a 1.8 to 4.3% fuel consumption reduction along a different drive cycle with TEG offering a 1.4% fuel saving on the WLTP on its own [34]. Kim et al. carried out an experiment to test the WHR performance of a TEG showing that the power produced by the TEG increases with engine load and speed. Moreover, a maximum power output of 119 W at 2000 rpm was achieved, as well as a maximum conversion efficiency of approximately 2.8% [35,36]. Lan et al. conducted a study to see how the location of the TEG affects the fuel economy potential in light-duty automotive applications. The study found that by placing a TEG closer to the exhaust manifold, the fuel-saving potential can increase by 50% [37].

Bang et al. studied the application of TEGs in medium-sized trucks. They found that these systems can save around 1.04 kL of fuel over 10 years, therefore justifying an economically acceptable cost of USD/kW 2905 for a TEG system [38,39]. This is significantly less than ORC systems due to the reduced complexity of the system. Moreover, Hendricks et al. carried out a cost analysis on an automotive TEG system using Skutterudite modules. They found that the most dominant components contributing to system costs are the heat exchangers used [40].

The aim of this study is to investigate the power recovery potential through the use of either ORC, sCO2, or TEG systems in automotive exhaust waste heat recovery applications in order to assess their suitability for automotive exhaust waste heat recovery systems. This will be achieved by completing the following objectives:

- Create a heavy-duty diesel engine model on GT-SUITE;
- Create TEG, ORC, and sCO2 system models on GT-SUITE and simulate these systems with the diesel engine model;
- Compare obtained results from simulations to relevant literature to come to a conclusion about which technology is most suitable for automotive exhaust waste heat recovery systems;
- The following sections include the Modelling Methodology in Section 2, where the heavy-duty diesel engine model is developed and described and then, in turn, the ORC, sCO2, and TEG models are, also, developed and described;
- In Section 3, the results for all three main waste heat recovery systems tested, are presented, as is their efficiency in improving the diesel engine's performance;
- Section 4 concludes with a summary of the main findings and purpose of this work.

2. Modelling Methodology

This work was carried out using the GT-SUITE software to model these systems. The software can be used to simulate the physics of fluid, mechanical, thermal, and electrical flow. The heavy-duty diesel engine, as well as the WHR systems, were built and simulated on GT-ISE using both the GT-POWER and the GT-SUITE components. Once this was completed, GT-POST, which is a post-processing tool than can quickly generate 2D and

3D plots from simulations, was used to analyze the results of the simulations as well as combine data from different cases. This section will describe in sufficient detail to allow repeatability, the creation of the diesel engine and WHR models that the results of this project are obtained from.

An important part of modelling in GT-SUITE is calibrating the different components in a system. In this project, the first step was to create standalone calibration models for the heat exchangers, compressors, pumps, and turbines used in the diesel engine and WHR models. These models were compared to reference test data provided by manufacturers of GT-SUITE for WHR applications, as well as other calibration data found in the literature. Once the components were calibrated and the quality of fit in comparison to test data was acceptable, the simulations for this project were initiated. The calibration data, as well as the key parameters for the design of the systems, can be found in the 'Appendices A–C' section of the report.

2.1. Heavy-Duty Diesel Engine Modelling

The engine used for this project is a 4-stroke, 6-cylinder, 11.7 L diesel engine with a compression ratio of 16:1. This is representative of typical engines that are currently used, for example, in heavy-duty trucks. The overall engine model can be seen in Figure 5. The modifications that were carried out on the base engine will be discussed below.

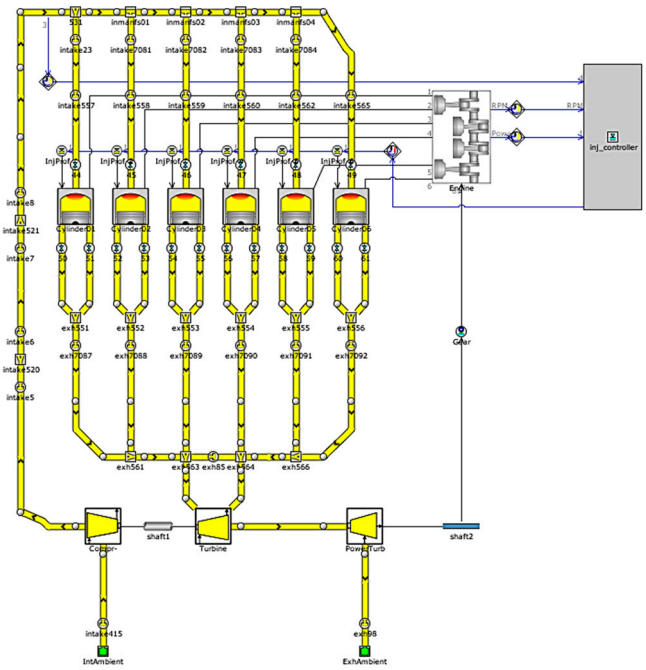

Figure 5. 6-Cylinder, 4-stroke, 11.7 L heavy-duty modified diesel engine model in GT- SUITE.

The engine cylinder temperatures are specified and can be changed for different scenarios in Table 1. The in-cylinder heat transfer model used in this study is the 'WoschniGT' model. This model uses a formula that closely emulates the classical Woschni correlation without swirl. However, the difference lies in the treatment of the heat transfer coefficients while the valves are open. The 'WoschniGT' model accounts for the heat transfer increased by inflow velocities through intake valves, as well as the backflow through the exhaust valves. Furthermore, the combustion model used is the direct injection (DI), three-term Wiebe function, which can be used when the fuel is injected directly into the cylinder. The DI-Wiebe function attempts to model the burn rate of diesel combustion by summing up three separate curves: a main curve, a premixed curve, and a tail curve. The chosen properties of the combustion model and heat transfer model can be found in Appendix A.

Table 1. Heavy-duty diesel engine specifications modelled in GT-SUITE.

Parameter	Value
Engine type	11.7 L, inline, 6-cylinder, 4-stroke Turbocharged diesel
Bore x stroke (mm)	119 × 175
Compression ratio	16:1
Connecting rod length (mm)	300
Maximum brake power (kW)	305–1800 rpm
Maximum torque (N·m)	1540–1400 rpm
Engine firing order	1-5-3-6-2-4
Head temperature (K)	570
Piston temperature (K)	600
Cylinder temperature (K)	480

In this model, the brake power from the engine is controlled by the amount of fuel injected into the cylinders. This brake power target, as well as the injected mass of fuel, is specified in the case setup section. Fueling is limited within the controller by an air-fuel ratio limit. Furthermore, the turbocharger adds a new dimension to the model, especially in regards to the convergence of the simulation. In general, the turbocharger can take a while to reach a steady speed even after flow convergence. Therefore, the turbocharger compressor and turbine need to be mapped accordingly. The desired turbocharger speed (in rpm) is defined by the user for the application in question. The compressor and turbine calibration data can both be found in Appendix A.

Once all of the necessary parameters are defined, the user can enter all of the relevant inputs needed for their simulation. In this project, the values chosen can be seen in Table 2. The final obtained results for the simulation can be found in the 'Results and Discussion' section of the report. Below, 'RPM' stands for 'revolutions per minute.

Table 2. Final chosen parameters for heavy-duty diesel engine model in GT-SUITE.

Parameter	Case 1	Case 2	Case 3	Case 4	Case 5	Case 6	Case 7	Case 8
Brake power target (KW)	240	270	295	305	270	225	155	90
Injected mass of fuel (mg)	255	240	225	210	195	180	165	150
Number of Cycle	75	75	75	75	75	75	75	75
RPM (rpm)	3000	2400	2000	1800	1600	1400	1200	1000
Turbocharger (rpm)	90,000	86,000	80,000	82,000	77,000	69,000	60,000	52,000

2.2. ORC System Modelling

The indirect integration study approach will be adopted in this study. This is where the engine is simulated separately from the WHR model. Firstly, the heavy-duty diesel engine model is simulated, and the results are stored in a database alongside boundary conditions. After this, the relevant data are inserted into the separate WHR model and simulated to obtain the power recovered by the system. The advantage of this approach is the faster solution times achievable relative to the direct method where the engine and WHR system are coupled together and solved simultaneously.

The ORC system model that was created for this project can be seen in Figure 6. This model incorporates typical components of an ORC system but has the added benefit of a recuperator to help further improve system efficiency. For this system, the working fluid that was selected was R245fa. Working fluid selection was based on practicality (availability of R245fa and cost). The point of the study was the comparison of three systems on a common basis and not an extensive investigation of optimal working fluids. In this model, the values for the exhaust gas mass flow rate can be specified by the user in the case setup section. These values were obtained from the diesel engine simulations that provided the indirect approach link between the engine and the WHR system as described previously.

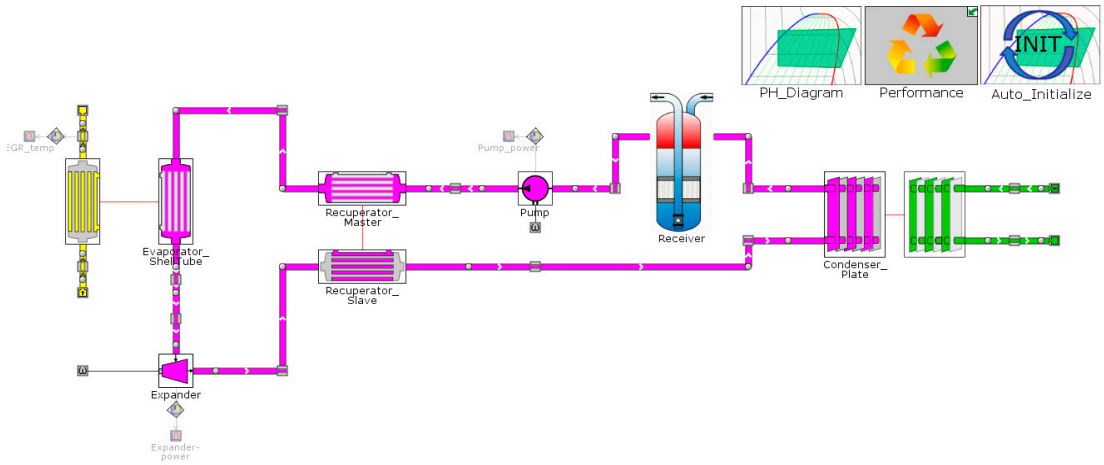

Figure 6. Schematic of the ORC system model and components layout in GT-SUITE.

After the ORC model is completed, the run setup needs to be defined. The time control flag is set to continuous for this simulation. Periodic time control would only be used if the WHR system was coupled with a GT-POWER engine. However, as discussed earlier, the indirect approach was taken in this project. The final parameters defined in the case setup for this simulation can be seen in Table 3. Note that only three cases are run in the WHR simulations. The reason for this will be discussed later in the 'Results and Discussion' section of the report. In Table 3, 'MFR' stands for 'Mass Flow Rate' and 'VFR' for 'Volume Flow Rate'.

Table 3. Final chosen parameters for the ORC system model on GT-SUITE.

Parameter	Case 1	Case 2	Case 3
Pump speed (rpm)	2000	2200	2400
Expander speed (rpm)	1350	1500	1650
Exhaust gas MFR (kg/s)	0.1369	0.3235	0.4770
Exhaust gas inlet temperature (K)	655.6	711.8	783.9
Condenser coolant VFR (L/min)	180	190	200
Coolant inlet temperature (°C)	26.85	26.85	26.85
Refrigerant initial temperature (°C)	26.85	26.85	26.85

2.3. sCO2 System Modelling

Figure 7 shows the sCO2 system model that was created in GT-SUITE for this project. The design of the system was based on the recuperated closed-loop Brayton cycle design that can be seen in the literature review. This system, as the ORC system designed, has the added benefit of increasing overall system efficiency by using a recuperator. The working fluid for this system is carbon dioxide (CO_2) in a supercritical state. In this state, the temperature and pressure of CO_2 is higher than its critical point and so the liquid and vapor phases are indistinguishable. This occurs when the temperature is higher than 31 °C and pressure is higher than 83.8 bar.

Once the system is modelled, the case setup section can be defined. The final case setup parameters can be seen in Table 4 below. One important parameter is the refrigerant initial temperature. This is set to 31 °C to ensure that the CO_2 is in a supercritical state throughout the entire system. Additionally, in the fluid properties for the model, the option to calculate properties above the supercritical pressure was chosen. The results of the simulation can be seen in the 'Results and Discussion' section of this report.

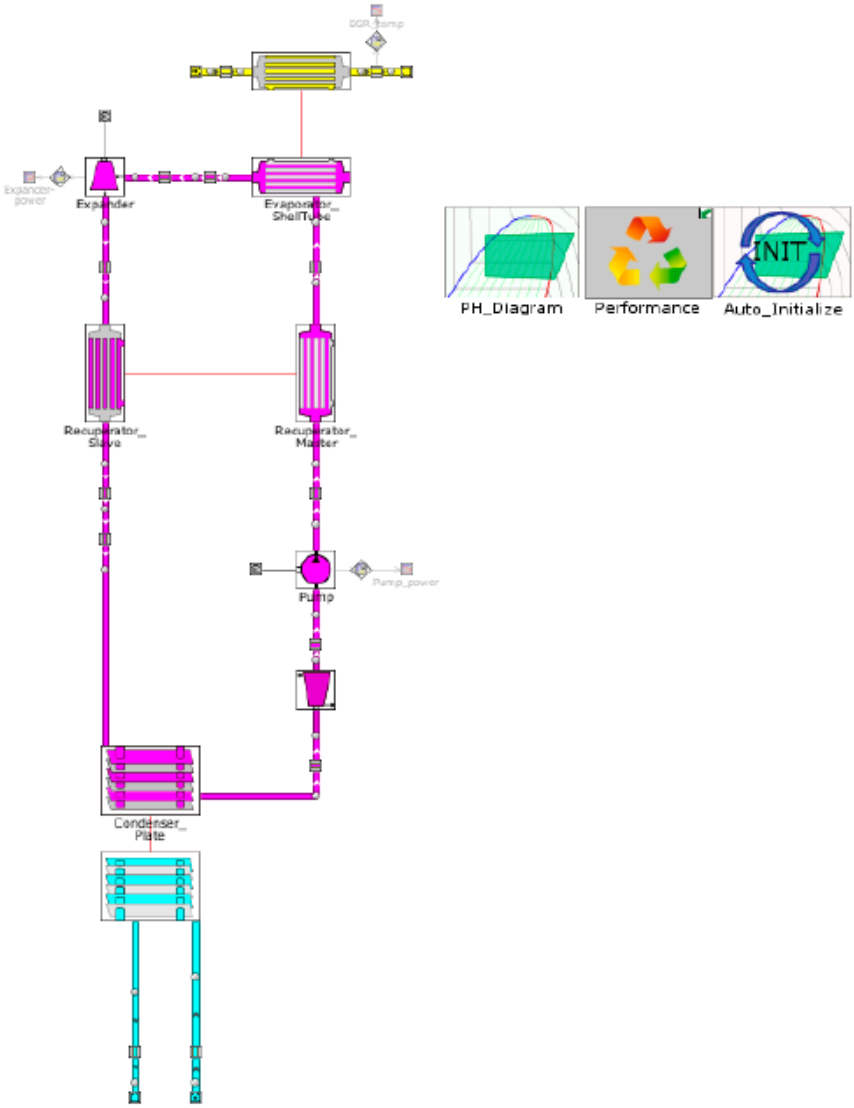

Figure 7. Schematic of the sCO2 system model in GT-SUITE.

Table 4. Final chosen parameters for the sCO2 system model in GT-SUITE.

Parameter	Case 1	Case 2	Case 3
Pump speed (rpm)	2000	2200	2400
Expander speed (rpm)	1350	1500	1650
ExhGas_MFR (kg/s)	0.13693	0.32345	0.47707
ExhGas inlet temperature (K)	655.5935	711.7872	783.91376
Condenser coolant VFR (L/min)	180	190	200
Coolant inlet temperature (°C)	26.85	26.85	26.85
Refrigerant initial temperature (°C)	31	31	31

2.4. TEG System Modelling

The final system being tested in this project is the TEG system that can be seen in Figure 8. A close up of the thermoelectric modules (TEM) can be seen in Figure 9. In this model, 10 TEM elements are sandwiched between a hot and a cold pipe. Each TEM connects thermally to the pipe walls such that a temperature difference exists across each TEM. The temperature difference produces a voltage within the TEM and therefore a current through the attached external electric circuit. The exhaust gas inlet properties (exhaust mass flow rate and temperature) are defined by the user in the case setup, alongside the pressure of the exhaust at the outlet.

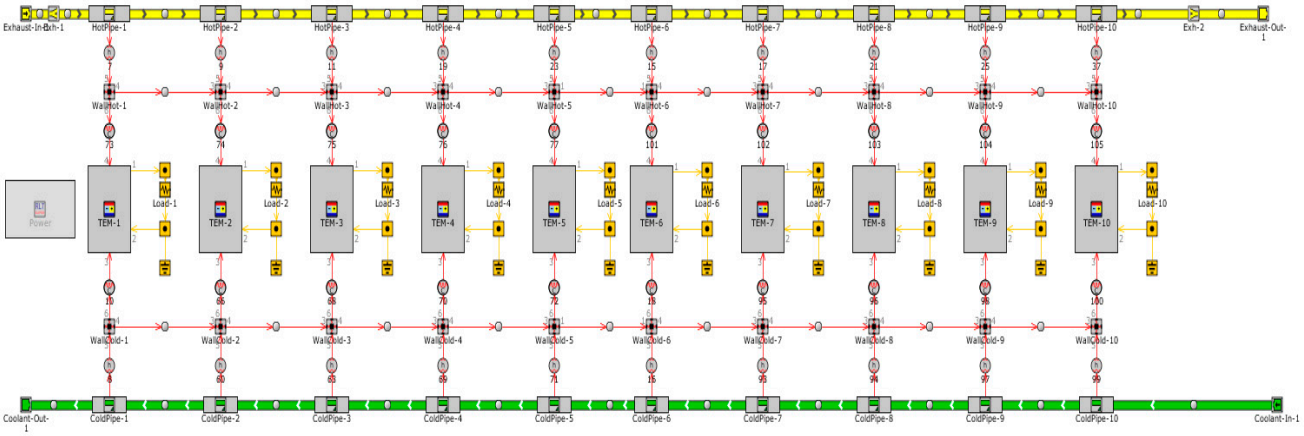

Figure 8. TEG system model in GT-SUITE.

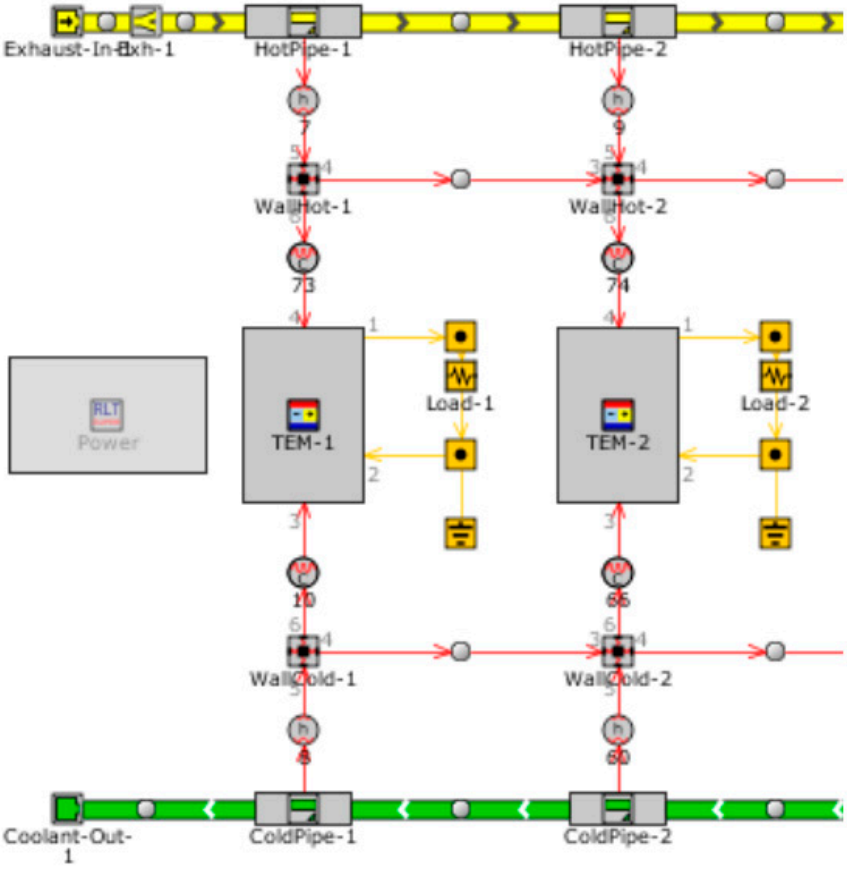

Figure 9. Schematic of TEG system close up.

Each pipe is modelled as a 'flat plate' that would be found in a typical plate-style heat exchanger. The pipes are modelled using thermal pipes connected to masses to represent the pipe walls (and fins for the inner pipe). Furthermore, the TEM template used in the model accounts for all three thermoelectric effects (Seebeck, Peltier, and Thomson) to generate an electric potential in response to a temperature difference across it. The same process is repeated for all 10 TEMs to obtain the complete model. To analyze the amount of power produced by the whole TEG system, an RLT creator part was made, which sums up all of the power outputs from each TEM. The final parameters in the case setup can be seen in Table 5 below.

Table 5. Final chosen parameters for TEG model in GT-SUITE.

Parameter	Case 1	Case 2	Case 3
Coolant mass flow rate (kg/s)	0.1	0.4	0.8
Exhaust mass flow (kg/s)	0.13693	0.32345	0.47707
Coolant outlet pressure (bar)	1	1	1
Exhaust outlet pressure (bar)	1.009656	1.0482228	1.0881422
coolant inlet temperature (°C)	25	25	25
Exhaust inlet temperature (K)	655.5935	711.7872	783.91376

3. Results and Discussion

After modelling the diesel engine and waste heat recovery systems, the results are analyzed and discussed in this section. In the first part, diesel engine modelling results are presented, and then waste heat recovery modelling is discussed.

3.1. Heavy-Duty Diesel Engine Model Results

Figure 10 shows the brake power produced by the heavy-duty diesel engine model from 1000 rpm to 3000 rpm. It can be seen that the maximum brake power produced by the engine is around 305 kW at 1800 rpm. This type of power is representative of current heavy-duty diesel engines. Moreover, the actual shape of the power curve and the rev range that it is produced at further increases confidence in the model. Similarly, in Figure 11 the brake torque produced by the engine in the same rpm range can be seen. We can see that the maximum brake torque produced is approximately 1540 N·m at 1400 rpm. Again, this figure at this power range is representative of current production heavy-duty diesel engines, thereby further increasing confidence in the model.

After obtaining the power and torque curves from the engine, it is important to select a few important points of operation in order to study how much power WHR systems can recover during typical driving scenarios. In this project, three points of operation were selected:

- Case 1. Point of low power and torque (90 kW brake power)—1000 rpm was selected as another point of interest;
- Case 2. Point of maximum torque (225 kW brake power)—1540 N·m was produced at 1400 rpm;
- Case 3. Point of maximum power (305 kW brake power)—305 kW was produced at 1800 rpm from the model.

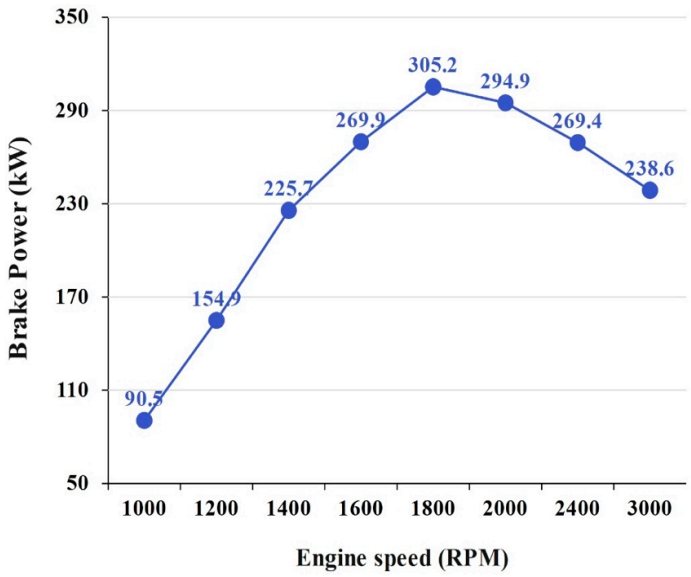

Figure 10. Brake power (kW) vs. engine speed (RPM) curve.

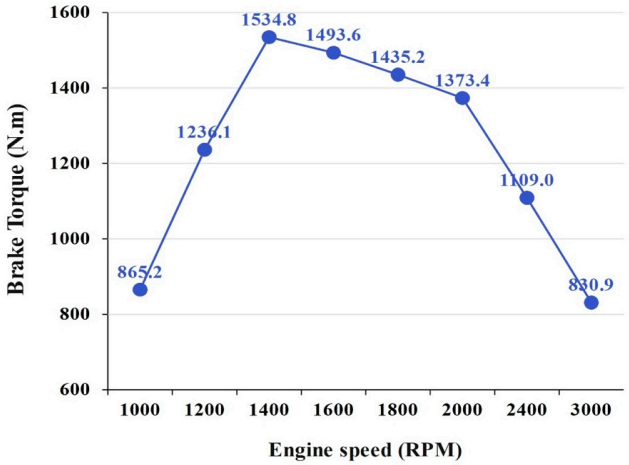

Figure 11. Brake torque (N·m) vs. engine speed (RPM) curve.

Figure 12 shows the exhaust mass flow rate for the 1000 rpm to 3000 rpm range. However, not all the points are of interest in this study as discussed above. Figure 13 shows the exhaust mass flow rates at the selected points of interest (1000 rpm, 1400 rpm, and 1800 rpm). This, alongside the exhaust temperature values at the points of interest in Figure 14, were entered into the WHR models as the exhaust input values. This is the reason why three cases are being run in the WHR models, as each case represents one point of interest. By obtaining these exhaust values, the indirect approach was taken as discussed in the 'Methodology' section of the report.

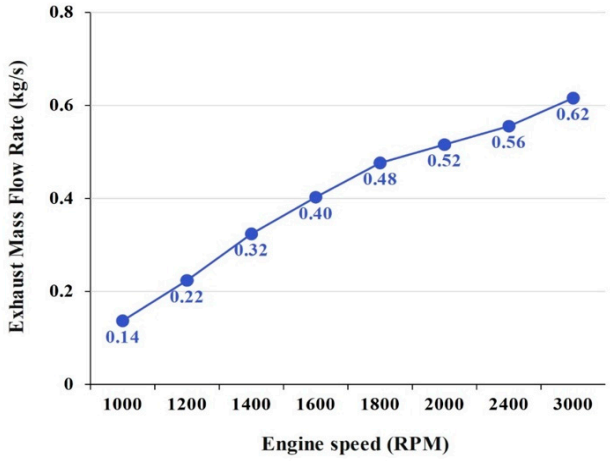

Figure 12. Exhaust mass flow rate (kg/s) vs. engine speed (RPM).

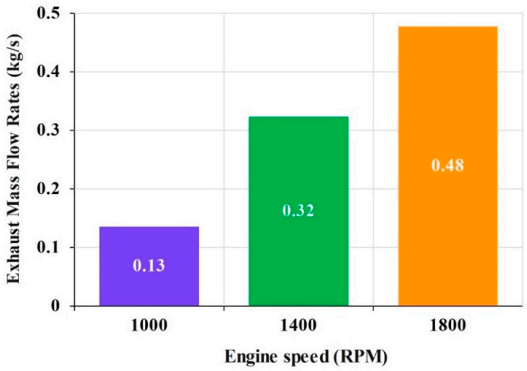

Figure 13. Exhaust mass flow rates for selected points of interest.

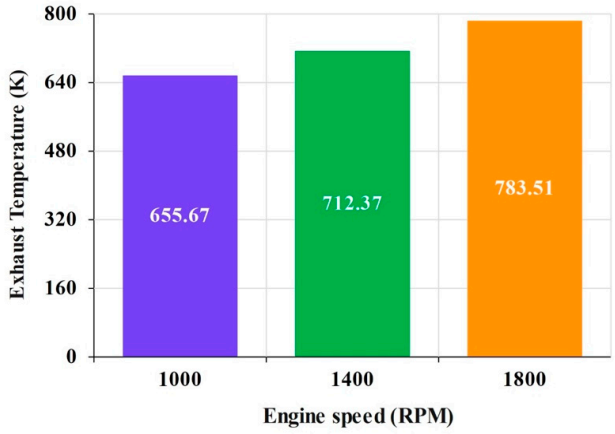

Figure 14. Exhaust temperature for selected points of interest.

3.2. WHR Systems Results

Figure 15 shows the expander power obtained at the selected points of interest. Note that in all of the WHR simulations, case number 1 represents the low power and torque point, case number 2 represents the point of maximum torque, and case number 3 represents the point of maximum power. We can see that at 1000 rpm, the ORC system was able to produce 3.3 kW of power. Furthermore, at the point of maximum torque, the ORC system was able to produce 7.9 kW of power. Lastly, at the point of maximum power, the ORC system produced 14.7 kW of power. These results are similar to previous studies carried out on similar engines, such as Teng et al.'s experiment on a Cummins ISX heavy-duty diesel engine and Pesyridis et al.'s ORC simulation on a 10.3 L, 316 kW turbocharged heavy-duty diesel engine (as discussed earlier in the literature review). Furthermore, these results fall in the simulation range that Xu et al. mentioned when they carried out an extensive study on all ORC WHR research undertaken so far. Therefore, we can be fairly confident in the results from the ORC model made on GT-SUITE as it is supported heavily by previous literature and a good working model. The efficiency of the ORC system is highly dependent on the working fluid selected. In this study, the working fluid that was chosen was R245fa. This is because R245fa is a well-established working fluid for ORC application with many desirable properties for ORC applications. For example, it has no ozone impact, low global warming potential, it is non-flammable, and it has the appropriate thermodynamic properties for WHR applications.

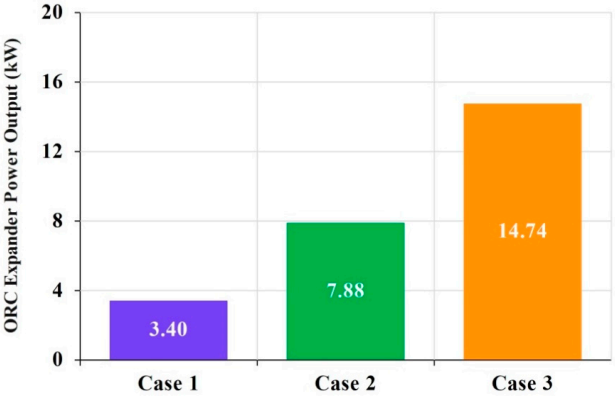

Figure 15. ORC expander power output (kW) vs. case number.

Figure 16 shows the expander power output for the sCO2 system at the selected points of interest. At the point of low power and torque (1000 rpm), the sCO2 system produced 4.1 kW of power. At 1400 rpm (maximum torque), the system produced 10.1 kW of power. Lastly, at the point of maximum power (1800 rpm), the system produced 19.5 kW.

In comparison to the ORC system results, we can see that at each point of interest, the sCO2 system produced more power. This is because sCO2 systems have higher efficiency than ORC systems, which is apparent in the results of this simulation.

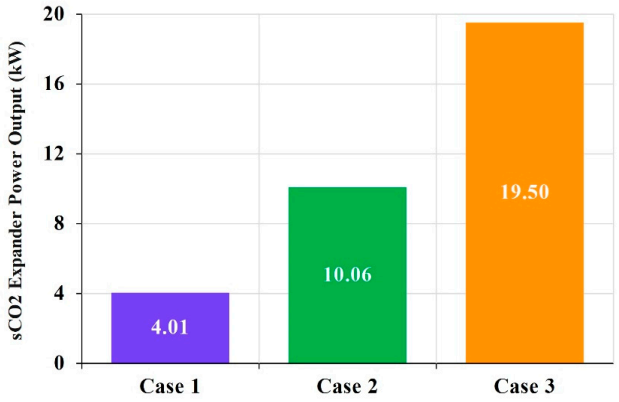

Figure 16. sCO2 expander power output (kW) vs. case number.

The final WHR system investigated in this project is the TEG system. In Figure 17, we can see the total power output from all 10 TEMs. At 1000 rpm, the system produced 7 W of power. At 1400 rpm, the system produced 126 W of power. Lastly, at 1800 rpm the system produced 533 W of power. In comparison to both the ORC and the sCO2 systems, the total power produced by the TEG system is significantly less. This is because TEGs have very low efficiency. In terms of the model, we can be confident that the model created on GT-SUITE is representative of current TEG technology as the results from the simulation are very similar to the literature in the field.

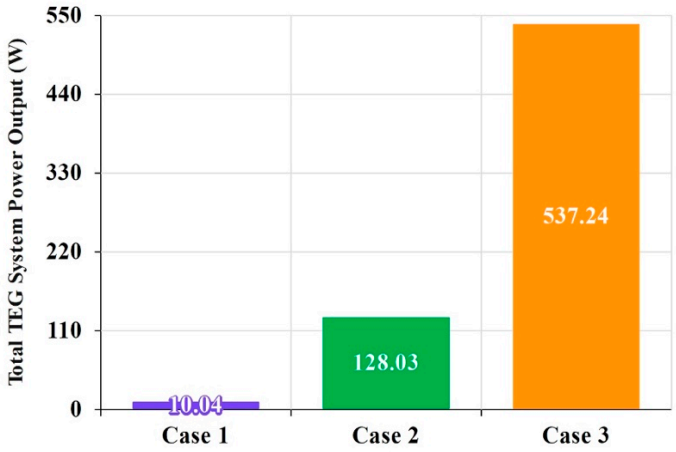

Figure 17. TEG system power output vs. case number.

Overall, from the results of all three WHR systems, in the Figure 18, it can be seen that the most likely systems to be successful for exhaust waste heat recovery applications for heavy-duty diesel engines are the ORC and sCO2 systems. These two systems have significantly higher efficiencies than TEGs and therefore recover much more power from the exhaust gases. Furthermore, sCO2 systems have the added benefit of being more compact due to the higher working pressures of the system. However, the main challenges facing both ORC and sCO2 systems are designing high efficiency turbines that are reliable at elevated pressures and temperatures. If these challenges can be overcome though, there is a significant opportunity for these systems to be adopted for WHR applications on a mass scale.

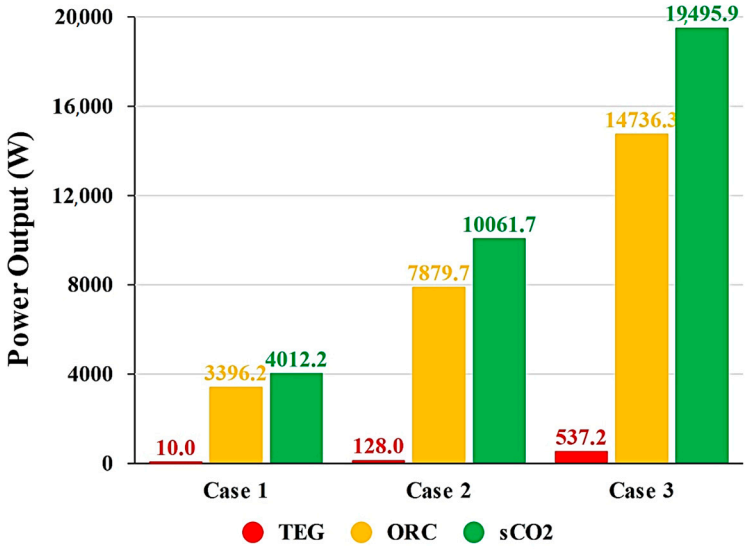

Figure 18. Comparison of three WHR systems.

Overall, this is the only study to consider all three main heat recovery systems for mobile application. Previous studies discussed from the literature (refer to [34]) stop short of implementing sCO2. Therefore, the value of this study lies in the concurrent assessment of these three principal options for waste heat recovery in a single study and carried out against a common comparative basis.

4. Conclusions

The aim of this study was to investigate the potential of ORC, sCO2, and TEG systems for use in heavy-duty diesel engine exhaust WHR. There was a number of simulations and experimental studies carried out on these systems for a wide variety of applications; however, they are yet to be adopted on a mass scale in transportation.

The results of the simulations showed that sCO2 systems are capable of recovering the most power from exhaust gases, followed closely by ORC systems. The sCO2 system recovered 19.5 kW at the point of maximum brake power and 10.1 kW at the point of maximum torque. Similarly, the ORC system recovered 14.7 kW at the point of maximum brake power and 7.9 kW at the point of maximum torque. Furthermore, at a point of low power and torque, the sCO2 system recovered 4.2 kW of power and the ORC system recovered 3.3 kW. The TEG system produced significantly less power (533 W at maximum brake power, 126 W at maximum torque, and 7 W at low power and torque) at all three points of interest due to the low system efficiency in comparison to sCO2 and ORC systems. Based on these results, we can be confident in proposing the theoretical viability of sCO2 and ORC systems as the most likely systems to be adopted for diesel engine WHR applications. The sCO2 systems have the highest efficiency of the three WHR systems and also have the benefit of being more compact due to the higher working pressures. Furthermore, the cost per kW of power produced by sCO2 systems is also significantly less than both ORC and TEG systems. Of course, the applicability of such systems is still a matter of debate in the context of the electrification of transportation, but the increasing introduction of alternative fuels and of hydrogen options means that such systems can be considered with renewed vigor. Obviously, there are still some challenges to be overcome in terms of component design and affordability of the systems for mass-scale production. However, if this is achieved, in the near term, the potential of these systems can be exploited. The energy recovered by these systems can be used to power auxiliary components, such as the air conditioning or lights, therefore reducing the fuel consumption of the vehicle. With growing pressure on automotive manufacturers to reduce emissions from their vehicles, these WHR systems could prove to be an attractive prospect. While in industrial use, SCO2 and ORC systems would require increased maintenance requirements compared to

TEG systems; in the transportation context, these requirements are likely to be minimal by design, but their evaluation was, in fact, out of the scope of this investigation.

Author Contributions: Data curation, Investigation, Writing-original draft, M.A.; Conceptualization, Data curation, Investigation, A.P.; Writing-original draft, J.A.S.; Supervision, Methodology, Validation, Writing-review & editing, A.M.A.; Supervision, Methodology, Writing-review & editing, A.G.; Supervision, Resources, Writing-review & editing, S.R. All authors have read and agreed to the published version of the manuscript.

Funding: This research received no external funding.

Data Availability Statement: Data available on request due to privacy.

Conflicts of Interest: The authors declare no conflict of interest.

Nomenclature

Abbreviation	Description
sCO2	Supercritical carbon dioxide
TEG	Thermoelectric generator
TEM	Thermoelectric modules
WHR	Waste heat recovery
RPM	Revolution per minute
ORC	Organic Rankine cycle
GHG	Greenhouse gas
GWP	Global warming potential
ODP	Ozone-depleting potential
Ref. In Temp.	Refrigerant initial temperature
ExhGas_MFR	Exhausr gas mass flow rate
ExhGas In Temp.	Exhaust gas inlet temperature
Cool_MFR	Coolant mass flow rate
Cool_Out_P	Coolant outlet pressure
Exh_Out_P	Exhaust outlet pressure

Appendix A

Heavy-Duty Diesel Engine Model Design Parameters on GT-SUITE.

Table A1. Engine cylinder heat transfer properties.

Parameter	Value
Heat transfer model	WoschniGT
Overall convection multiplier	1
Head/bore area ratio	1
Piston/bore area ratio	1.3
Radiation multiplier	1

Table A2. DI Wiebe combustion model properties.

Parameter	Value
Premixed fraction	0.017
Ignition delay	2
Tail fraction	0.05
Premixed duration	2
Main duration	33
Tail duration	45
Premixed exponent	0.7
Main exponent	1.1
Tail exponent	1.3

Table A3. Compressor calibration data.

Attribute	Speed (RPM)	Mass Flow Rate (kg/s)	Pressure Ratio	Efficiency (Fraction)
1	55,984	0.15	1.75	0.67
2	55,984	0.2113	1.703	0.737
3	55,984	0.3769	1.669	0.763
4	55,984	0.3333	1.608	0.735
5	55,984	0.3948	1.494	0.639
6	73,974	0.23	2.42	0.68
7	73,974	0.3119	2.382	0.74
8	73,974	0.3871	2.348	0.771
9	73,974	0.4586	2.225	0.745
10	73,974	0.5283	1.969	0.639
11	88,485	0.36	3.21	0.69
12	88,485	0.4388	3.191	0.746
13	88,485	0.4869	3.152	0.758
14	88,485	0.5468	2.963	0.731
15	88,485	0.5975	2.536	0.635
16	102,000	0.44	4.022	0.7
17	102,000	0.52	4.018	0.709
18	102,000	0.5455	3.967	0.712
19	102,000	0.58	3.785	0.7
20	102,000	0.63145	3.223	0.631

Table A4. Turbine calibration data.

Attribute	Speed (RPM)	Mass Flow Rate (kg/s)	Pressure Ratio (bar)	Efficiency (fraction)
1	40,700	0.25	1.27	0.76
2	40,700	0.276	1.31	0.8
3	40,700	0.2888	1.349	0.831
4	40,700	0.294	1.38	0.81
5	49,700	0.295	1.46	0.79
6	49,700	0.32	1.53	0.83
7	49,700	0.3223	1.594	0.846
8	49,700	0.338	1.63	0.823
9	57,300	0.343	1.75	0.821
10	57,300	0.349	1.83	0.847
11	57,300	0.3553	1.882	0.856
12	64,000	0.3573	1.92	0.846
13	64,000	0.348	2.02	0.838
14	64,000	0.355	2.09	0.855
15	64,000	0.3629	2.161	0.863
16	70,000	0.366	2.23	0.849
17	70,000	0.353	2.31	0.825
18	70,000	0.357	2.36	0.842
19	70,000	0.3606	2.416	0.854
20	102,000	0.363	2.5	0.847

Appendix B

ORC and sCO2 System Model Design Parameters on GT-SUITE.

Table A5. Evaporator heat exchanger specifications.

Attribute	Value
Tube length (mm)	850
Inlet connection diameter (master fluid) (mm)	12.7
Outlet connection diameter (master fluid) (mm)	117.0973
Number of tubes	100
Inlet tank volume (L)	0.03335
Outlet tank volume (L)	0.03335
Dry mass of heat exchanger material (kg)	10
Heat exchanger material properties object	Stainless steel

Table A6. Evaporator heat transfer calibration data.

Attribute	Master Inlet Temperature (°C)	Master Inlet Static Pressure (bar)	Master Outlet Static Pressure (bar)	Master Mass Flow Rate (kg/s)	Slave Inlet Temperature (°C)	Slave Inlet Static Pressure (bar)	Slave Outlet Static Pressure (bar)	Slave Mass Flow Rate (kg/s)	Heat Transfer Rate (kW)
1	45	20.0025	20	0.1	700	1.00074	1	0.05	28.8
2	45	20.0072	20	0.2	700	1.00232	1	0.08	47.1
3	45	20.0202	20	0.3	700	1.00747	1	0.14	82.8
4	45	20.0313	20	0.4	700	1.01074	1	0.17	98.8
5	45	20.0521	20	0.5	700	1.01973	1	0.23	130

Table A7. Expander calibration data.

Attribute	Turbine Speed (RPM)	Volumetric Efficiency (Fraction)	Suction Pressure (bar)	Suction Temperature (°C)	Discharge Pressure (bar)	Discharge Temperature (°C)	Total Shaft Power Output (kW)
1	1000	0.92	20	150	10	127.6	1.39
2	1000	0.94	20	150	7	122.13	2.12
3	1000	0.95	20	150	5	117.85	4.48
4	1000	0.95	20	150	2.5	109.47	3.41
5	2000	0.73	20	150	10	127.7	2.71
6	2000	0.75	20	150	7	121.62	3.89
7	2000	0.75	20	150	5	116.61	4.67
8	2000	0.76	20	150	2.5	112.13	5.31
9	3000	0.63	20	150	10	129.4	3.58
10	3000	0.64	20	150	7	123.02	4.74
11	3000	0.65	20	150	5	117.77	5.85
12	3000	0.65	20	150	2.5	116.52	5.61
13	4000	0.55	20	150	10	132.43	3.05
14	4000	0.56	20	150	7	125.67	4.55
15	4000	0.56	20	150	5	121.11	5.75
16	4000	0.56	20	150	2.5	121.11	4.84

Table A8. Recuperator heat exchanger specifications.

Attribute	Value
Tube length (mm)	600
Inlet connection diameter (master fluid) (mm)	12.7
Outlet connection diameter (master fluid) (mm)	12.7
Number of tubes	1
Inlet tank volume (L)	0.1
Outlet tank volume (L)	0.1
Dry mass of heat exchanger material (kg)	5
Heat exchanger material properties object	Aluminum

Table A9. Recuperator heat transfer calibration data.

Attribute	Master Inlet Temperature (°C)	Master Inlet Static Pressure (bar)	Master Outlet Static Pressure (bar)	Master Mass Flow Rate (kg/s)	Slave Inlet Temperature (°C)	Slave Inlet Static Pressure (bar)	Slave Outlet Static Pressure (bar)	Slave Mass Flow Rate (kg/s)	Heat Transfer Rate (kW)
1	318	26	26	0.15	355	2.9	2.9	0.15	5.36585
2	318	26	26	0.2	355	2.9	2.9	0.2	7.07691
3	318	26	26	0.25	355	2.9	2.9	0.25	8.7795
4	318	26	26	0.3	355	2.9	2.9	0.3	10.4803

Table A10. Condenser heat exchanger specifications.

Attribute	Value
Plate length (mm)	200
Plate width (mm)	200
Connection diameter (master fluid) (mm)	75.2892
Connection diameter (slave fluid) (mm)	60
Number of channels (master fluid)	12
Number of channels (slave fluid)	11
Dry mass of heat exchanger material (kg)	3.8
Heat exchanger material properties object	Aluminum

Table A11. Condenser heat transfer calibration data.

Attribute	Master Inlet Temperature (°C)	Master Inlet Static Pressure (bar)	Master Outlet Static Pressure (bar)	Master Mass Flow Rate (kg/s)	Slave Inlet Temperature (°C)	Slave Inlet Static Pressure (bar)	Slave Outlet Static Pressure (bar)	Slave Mass Flow Rate (kg/s)	Heat Transfer Rate (kW)
1	70	3.22	3.2	0.1	23	2.01856	2	40	20.6910
2	70	3.25	3.2	0.2	23	2.07423	2	80	41.3821
3	70	3.3	3.2	0.3	23	2.167	2	120	62.0732
4	70	3.35	3.2	0.4	23	2.29687	2	160	82.7643
5	70	3.41	3.2	0.5	23	2.46384	2	200	103.4554

Table A12. Pump calibration data.

Attribute	Speed (RPM)	Volumetric Flow Rate (m^3/s)	Pressure Ratio (bar)	Total Isentropic Efficiency (Fraction)
1	1000	8.25×10^{-5}	29	0.48
2	1000	9.3×10^{-5}	25	0.51
3	1000	9.76×10^{-5}	23	0.53
4	1000	1.12×10^{-4}	15	0.54
5	1000	1.15×10^{-4}	13	0.55
6	1000	1.24×10^{-4}	17	0.58
7	1500	1.2×10^{-4}	29	0.52
8	1500	1.36×10^{-4}	25	0.57
9	1500	1.41×10^{-4}	23	0.61
10	1500	1.63×10^{-4}	15	0.63
11	1500	1.67×10^{-4}	13	0.64

Appendix C

TEG System Model Design Parameters on GT-SUITE.

Table A13. TEG model hot and cold pipe properties.

Parameter	Hot Pipe Value	Cold Pipe Value
The area at inlet end (mm^2)	5.26	500
Wetted perimeter at inlet end (mm)	12.1	210
The area at outlet end (mm^2)	5.26	500
Wetted perimeter at outlet end (mm)	12.1	210
Length (mm)	50	50
Discretization length (mm)	50	50
Number of identical pipes	80	1

Table A14. TEG model hot and cold thermal block properties.

Parameter	Hot Thermal Block	Cold Thermal Block
Material properties object	Aluminum	Aluminum
Mass (g)	40	29
Height (mm)	2	2
Length (mm)	50	50
Width (mm)	100	100

References

1. Song, J.; Ren, X.-D.; Gu, C.-W. Investigation of Engine Waste Heat Recovery Using Supercritical CO_2 (S-CO_2) Cycle System. In *Turbo Expo: Power for Land, Sea, and Air*; American Society of Mechanical Engineers: New York, NY, USA, 2018; Volume 51180, p. V009T38A014.
2. Olabi, A.B.; Al-Murisi, M.; Maghrabie, H.M.; Yousef, B.A.A.; Sayed, E.T.; Alami, A.H.; Abdelkareem, M.A. Potential applications of thermoelectric generators (TEGs) in various waste heat recovery systems. *Int. J. Thermofluids* **2022**, *16*, 100249. [CrossRef]
3. Feneley, A.J.; Pesiridis, A.; Andwari, A.M. Variable geometry turbocharger technologies for exhaust energy recovery and boosting—A Review. *Renew. Sustain. Energy Rev.* **2017**, *71*, 959–975. [CrossRef]
4. Mahmoudzadeh Andwari, A.; Pesyridis, A.; Esfahanian, V.; Salavati-Zadeh, A.; Hajialimohammadi, A. Modelling and evaluation of waste heat recovery systems in the case of a heavy-duty diesel engine. *Energies* **2019**, *12*, 1397. [CrossRef]
5. Eichler, K.; Jeihouni, Y.; Ritterskamp, C. Fuel economy benefits for commercial diesel engines with waste heat recovery. *SAE Int. J. Commer. Veh.* **2015**, *8*, 491–505. [CrossRef]
6. Moradi, J.; Gharehghani, A.; Mirsalim, M. Numerical investigation on the effect of oxygen in combustion characteristics and to extend low load operating range of a natural-gas HCCI engine. *Appl. Energy* **2020**, *276*, 115516. [CrossRef]
7. Moradi, J.; Gharehghani, A.; Mirsalim, M. Numerical comparison of combustion characteristics and cost between hydrogen, oxygen and their combinations addition on natural gas fueled HCCI engine. *Energy Convers. Manag.* **2020**, *222*, 113254. [CrossRef]
8. Gharehghani, A.; Mirsalim, S.M.; Jazayeri, S.A. Numerical and Experimental Investigation of Combustion and Knock in a Dual Fuel Gas/Diesel Compression Ignition Engine. *J. Combust.* **2012**, *2012*, 504590. [CrossRef]
9. Gharehghani, A.; Kakoee, A.; Andwari, A.M.; Megaritis, T.; Pesyridis, A. Numerical Investigation of an RCCI Engine Fueled with Natural Gas/Dimethyl-Ether in Various Injection Strategies. *Energies* **2021**, *14*, 1638. [CrossRef]
10. Mehranfar, S.; Gharehghani, A.; Azizi, A.; Mahmoudzadeh Andwari, A.; Pesyridis, A.; Jouhara, H. Comparative assessment of innovative methods to improve solar chimney power plant efficiency. *Sustain. Energy Technol. Assess.* **2022**, *49*, 101807. [CrossRef]
11. Guo, J.-Q.; Li, M.J.; He, Y.L.; Jiang, T.; Ma, T.; Xu, J.L.; Cao, F. A systematic review of supercritical carbon dioxide(S-CO2) power cycle for energy industries: Technologies, key issues, and potential prospects. *Energy Convers. Manag.* **2022**, *258*, 115437. [CrossRef]
12. White, M.T.; Bianchi, G.; Chai, L.; Tassou, S.A.; Sayma, A.I. Review of supercritical CO_2 technologies and systems for power generation. *Appl. Therm. Eng.* **2021**, *185*, 116447. [CrossRef]
13. Kim, S.C.; Won, J.P.; Kim, M.S. Effects of operating parameters on the performance of a CO_2 air conditioning system for vehicles. *Appl. Therm. Eng.* **2009**, *29*, 2408–2416. [CrossRef]
14. Siddiqui, M.E.; Almatrafi, E.; Bamasag, A.; Saeed, U. Adoption of CO_2-based binary mixture to operate transcritical Rankine cycle in warm regions. *Renew. Energy* **2022**, *199*, 1372–1380. [CrossRef]
15. Siddiqui, M.E. Thermodynamic Performance Improvement of Recompression Brayton Cycle Utilizing CO_2-C7H8 Binary Mixture. *Mechanics* **2021**, *27*, 259–264. [CrossRef]
16. Wieland, C.; Schifflechner, C.; Dawo, F.; Astolfi, M. The organic Rankine cycle power systems market: Recent developments and future perspectives. *Appl. Therm. Eng.* **2023**, *224*, 119980. [CrossRef]
17. Manjunath, K.; Sharma, O.P.; Tyagi, S.K.; Kaushik, S.C. Thermodynamic analysis of a supercritical/transcritical CO_2 based waste heat recovery cycle for shipboard power and cooling applications. *Energy Convers. Manag.* **2018**, *155*, 262–275. [CrossRef]
18. Marchionni, M.; Bianchi, G.; Tsamos, K.M.; Tassou, S.A. Techno-economic comparison of different cycle architectures for high temperature waste heat to power conversion systems using CO_2 in supercritical phase. *Energy Procedia* **2017**, *123*, 305–312. [CrossRef]
19. Mahmoudi, A.; Fazli, M.; Morad, M. A recent review of waste heat recovery by Organic Rankine Cycle. *Appl. Therm. Eng.* **2018**, *143*, 660–675. [CrossRef]
20. Teng, H.; Regner, G.; Cowland, C. *Achieving High Engine Efficiency for Heavy-Duty Diesel Engines by Waste Heat Recovery Using Supercritical Organic-Fluid Rankine Cycle*; SAE Technical Paper, 0148-7191; SAE International: Warrendale, PA, USA, 2006.
21. Cipollone, R.; Di Battista, D.; Perosino, A.; Bettoja, F. *Waste Heat Recovery by an Organic Rankine Cycle for Heavy Duty Vehicles*; SAE Technical Paper, 0148-7191; SAE International: Warrendale, PA, USA, 2016.
22. Mahmoudzadeh Andwari, A.; Pesiridis, A.; Esfahanian, V.; Salavati-Zadeh, A.; Karvountzis-Kontakiotis, A.; Muralidharan, V. A comparative study of the effect of turbocompounding and ORC waste heat recovery systems on the performance of a turbocharged heavy-duty diesel engine. *Energies* **2017**, *10*, 1087. [CrossRef]

23. Mahmoudzadeh Andwari, A.; Pesiridis, A.; Karvountzis-Kontakiotis, A.; Esfahanian, V. Hybrid electric vehicle performance with organic rankine cycle waste heat recovery system. *Appl. Sci.* **2017**, *7*, 437. [CrossRef]
24. Arunachalam, P.N.; Shen, M.; Tuner, M.; Tunestal, P.; Thern, M. *Waste Heat Recovery from Multiple Heat Sources in a HD Truck Diesel Engine Using a Rankine Cycle—A Theoretical Evaluation*; SAE Technical Paper, 0148-7191; SAE International: Warrendale, PA, USA, 2012.
25. Varshil, P.; Deshmuk, D. A comprehensive review of waste heat recovery from a diesel engine using organic rankine cycle. *Energy Rep.* **2021**, *7*, 3951–3970.
26. Teng, H.; Klaver, J.; Park, T.; Hunter, G.L.; van der Velde, B. *A Rankine Cycle System for Recovering Waste Heat from HD Diesel Engines—WHR System Development*; SAE Technical Paper, 0148-7191; SAE International: Warrendale, PA, USA, 2011.
27. Laouid, Y.A.A.; Kezrane, C.; Lasbet, Y.; Pesyridis, A. Towards improvement of waste heat recovery systems: A multi-objective optimization of different organic Rankine cycle configurations. *SAE Int. J. Thermofluids* **2022**, *11*, 100100. [CrossRef]
28. Hoang, A.T. Waste heat recovery from diesel engines based on Organic Rankine Cycle. *Appl. Energy* **2018**, *231*, 138–166. [CrossRef]
29. Chintala, V.; Kumar, S.; Pandey, J.K. A technical review on waste heat recovery from compression ignition engines using organic Rankine cycle. *Renew. Sustain. Energy Rev.* **2018**, *81*, 493–509. [CrossRef]
30. Nawi, Z.M.; Kamarudin, S.; Abdullah, S.S.; Lam, S. The potential of exhaust waste heat recovery (WHR) from marine diesel engines via organic rankine cycle. *Energy* **2019**, *166*, 17–31. [CrossRef]
31. Mondejar, M.; Andreasen, J.; Pierobon, L.; Larsen, U.; Thern, M.; Haglind, F. A review of the use of organic Rankine cycle power systems for maritime applications. *Renew. Sustain. Energy Rev.* **2018**, *91*, 126–151. [CrossRef]
32. Xu, B.; Rathod, D.; Yebi, A.; Filipi, Z.; Onori, S.; Hoffman, M. A comprehensive review of organic rankine cycle waste heat recovery systems in heavy-duty diesel engine applications. *Renew. Sustain. Energy Rev.* **2019**, *107*, 145–170. [CrossRef]
33. Kumar, S.; Heister, S.D.; Xu, X.; Salvador, J.R.; Meisner, G.P. Thermoelectric generators for automotive waste heat recovery systems part II: Parametric evaluation and topological studies. *J. Electron. Mater.* **2013**, *42*, 944–955. [CrossRef]
34. Lan, S.; Li, Q.; Guo, X.; Wang, S.; Chen, R. Fuel saving potential analysis of bifunctional vehicular waste heat recovery system using thermoelectric generator and organic Rankine cycle. *Energy* **2023**, *263*, 125717. [CrossRef]
35. Kim, T.Y.; Negash, A.A.; Cho, G. Waste heat recovery of a diesel engine using a thermoelectric generator equipped with customized thermoelectric modules. *Energy Convers. Manag.* **2016**, *124*, 280–286. [CrossRef]
36. Andwari, A.M.; Pesiridis, A.; Esfahanian, V.; Muhamad Said, M.F. Combustion and emission enhancement of a spark ignition two-stroke cycle engine utilizing internal and external exhaust gas recirculation approach at low-load operation. *Energies* **2019**, *12*, 609. [CrossRef]
37. Lan, S.; Yang, Z.; Stobart, R.; Chen, R. Prediction of the fuel economy potential for a skutterudite thermoelectric generator in light-duty vehicle applications. *Appl. Energy* **2018**, *231*, 68–79. [CrossRef]
38. Bang, S.; Kim, B.; Youn, N.; Kim, Y.; Wee, D. Economic and environmental analysis of thermoelectric waste heat recovery in conventional vehicles operated in Korea: A model study. *J. Electron. Mater.* **2016**, *45*, 1956–1965. [CrossRef]
39. Andwari, A.M.; Said, M.F.M.; Aziz, A.A.; Esfahanian, V.; Salavati-Zadeh, A.; Idris, M.A.; Perang, M.R.M.; Jamil, H.M. Design, modeling and simulation of a high-pressure gasoline direct injection (GDI) pump for small engine applications. *J. Mech. Eng.* **2018**, *1*, 107–120.
40. Sivaprahasam, D.; Harish, S.; Gopalan, R.; Sundararajan, G. Automotive Waste Heat Recovery by Thermoelectric Generator Technology. In *Bringing Thermoelectricity into Reality*; IntechOpen: London, UK, 2018; pp. 163–182.